Modal Q Factor and Modal Overlap of Electrically Small Avionics Boxes

Paul G Bremner[1], Dawn Trout[2], Gabriel Vazquaz[2], Neda Nourshamsi[3], James C.West[3], Charles F. Bunting[3]

[1] *Robust Physics, Del Mar, CA 92014 USA, pbremner@robustphysics.com*
[2] *NASA Kennedy Space Center, Cape Canaveral, FL, USA, gabriel.vazquez@nasa.gov*
[3] *School of Electrical and Computer Engineering, Oklahoma State University, 202 ES, Stillwater, OK 74078, USA*
charles.bunting@okstate.edu

***Abstract*— Estimating the electromagnetic field strength in avionics boxes and other small enclosures at the design stage requires an estimate of the Q factor of the cavity modes. When the enclosure is small, it is typically under-moded so that Q measurement techniques which are standard practice in over-moded reverberation chambers may not be a robust measure. Furthermore, practical antenna used to measure Q in a small cavity may have a strong influence on the result obtained, as reported by Tait et al, IEEE Trans. EMC 55 2 2012. This paper reports the results of testing to determine the Q factor of a small aperture enclosure, used in a statistical power balance model to predict the electric field strength. The contributors to the total Q are identified. A novel S_{11} curve fitting method to measure modal Q is introduced and compared with the time domain method for measuring Q.**

Keywords*— *Statistical electromagnetics, Reverberant field, Q factor measurement

I. Introduction

The authors have a continuing interest in application of the statistical power balance methods proven in reverberation chambers [1] to the model-based prediction of electric field strength in electrically small spacecraft enclosures [3][4] and avionics boxes [5][6]. Characterizing the coupling in avionics sized boxes residing in cavities such as fairings or spacecraft environmental shelters provides insight into an analytical approach to verify immunity to high resonant fields from nearby emitters.

The electromagnetic resonance mode count (modal density) in small enclosures decreases with volume and frequency squared [1]. If the effective Q of the enclosure is large, then resonant modes in an electrically small enclosure will be well separated (ie. non-overlapping) in frequency, a condition referred to as "under-moded". It follows that under-moded cavities will require a large amount of mode-stirring for the statistical power balance principles of reverberation chambers to apply. And it is likely that the maximum expected electric field response in any *specific* (un-stirred, single instance) enclosure may not be predictable from the Rayleigh statistics models applicable to over-moded reverberation chambers [16][14][5][6]. It is therefore important to be able to measure and predict the Q factor of small enclosures.

Another issue is that measurement of Q in small enclosures requires the use of antennas which are small compared with enclosure dimensions. Compact monopole-type antennae do not have a good broadband power acceptance characteristic, due to impedance mismatch at frequencies removed from the antenna standing wave resonances [7]. The antenna power acceptance in a small enclosure can also be expected to be quite different to its free field characteristic, which would otherwise be a good approximation in an over-moded reverberation chamber [2]. Established frequency domain methods of measuring Q and shielding effectiveness in small enclosures therefore require a rather large impedance mismatch correction [7].

This paper reviews two Q factor measurement techniques and evaluates their application to a small box with different aperture losses. A new method to obtain Q using modal curve fitting is introduced and its potential use and consistency with other measurement techniques is demonstrated.

II. Modal Overlap

In a related study of the shielding effectiveness of electrically small enclosures, Tait [7] used the notion of "modal overlap" to describe the under-moded condition. The under-moded condition may not be fully defined by the mode count or the spacing of modes. Modal overlap $m(\omega)$ defined as the ratio of the modal damping bandwidth to the frequency spacing

$$m = \omega\eta n \equiv \omega n/Q \tag{1}$$

is a potentially more useful metric. The modal density n (s/rad) of the enclosure [1] with volume V is

$$n(\omega) = \frac{V\omega^2}{2\pi^2 c^3} \tag{2}$$

Modal overlap greater than unity is a sufficient condition for over-moded cavity statistics. Studies of test chamber loading to improve spatial uniformity of the electric field [15]

confirm that modal overlap – not just modal density – determine the electric field statistics.

In the analogous field of room acoustics [16], it has been shown that the statistics of reverberant wave fields are strongly dependent on modal overlap. Bremner [14] has confirmed that the low frequency statistics of reverberant chamber energy level (electric field averaged over the whole enclosure volume) can be predicted directly from modal overlap, using the variance formulations developed for acoustics.

III. Q Factor Measurement Methods

For a statistically uniform electric field in a well-stirred reverberation chamber, it has been shown [1] that the power balance principle applies

$$P_{in} = P_{diss} = \omega \eta_L U \equiv \omega U / Q \qquad (3)$$

The total power dissipated by all losses is equal to the fraction of power loss per radian η_L, times the field energy level $U = \varepsilon V \left\langle |E_T|^2 \right\rangle_{vol}$, occurring at rate ω (rad/s). The Q factor is the inverse of the loss factor $Q = \eta_L^{-1}$.

Two different Q factor measurement techniques were considered for this study.

A. *Time Domain T60 Energy Decay Time Method .*

In the time domain, the quality factor of the chamber is directly related to the decay rate of the energy within the chamber [10]. The bandwidth of the signal required to perform a measurement has been established by Nourshamsi et al [12].

The mean time response can be divided into two phases, the pre-reverberant phase, when the energy is injected into the reverberation chamber, and the reverberant phase, when the energy decay exponentially due to different losses inside the enclosure. The decay time can be calculated by averaging over tuner positions.

The chamber time constant is defined as [10]:

$$\tau = \frac{4.3429}{Slope \dfrac{dB}{\mu s}} \quad (\mu s) \qquad (4)$$

where the slope term is the slope of the mean chamber time-domain response in $dB/\mu s$ in the reverberant phase of the response. Typically, a linear regression is applied to the reverberant phase response in order to find the slope of the regression line. The chamber quality factor is defined [11]

$$Q = 2\pi f_c \tau, \qquad (5)$$

where f_c is the frequency at the center of the time-domain signal bandwidth. The mean time-domain response will usually be noisy even after averaging over multiple tuner positions.

B. *Modal Curvefitting Method*

Linearity and closure boundary conditions mean that each of the $\xi = x, y, z$ rectangular components of the electric field vector $E_\xi(\mathbf{x}, j\omega)$ can be represented in separable form by the sum of cavity modal responses [1], [13], [14]

$$E_\xi(\mathbf{x}, j\omega) = \frac{-j\omega L_d}{\varepsilon V} \sum_r \frac{\psi_r^T(\mathbf{x}_i, \xi) I_\xi(\mathbf{x}_i, j\omega) \psi_r(\mathbf{x}, \xi)}{\left[\omega_r^2(1 + j\eta_r) - \omega^2\right]} \qquad (6)$$

where $I_\xi(\mathbf{x}_i, j\omega)$ is the fluctuating current on a small dipole source of length L_d of orientation ξ at location $\mathbf{x}_i$. The *rth* resonant mode of the cavity has a natural frequency ω_r, modal damping loss factor η_r and mode shape $\psi_r(\mathbf{x}, \xi)$ defined over the whole cavity volume *V*

The power input P_{in} by the localized current source $I_\xi^2(x_i, \omega)$ can be expressed [14] as

$$P_{in}(\mathbf{x}_i, \omega) = \frac{L_d^2}{\varepsilon V} \sum_r \frac{\omega \eta_r \omega_r^2 \psi_r^2(\mathbf{x}_i, \xi) I_\xi^2(\mathbf{x}_i, \omega)}{\left[\left(\omega_r^2 - \omega^2\right)^2 + \eta_r^2 \omega_r^4\right]} \qquad (7)$$

When the small dipole current source result is integrated over the length of a straight wire antenna, it represents the power radiated by the antenna into the enclosure resonant modes. It follows that the measured $1 - |\langle S_{11} \rangle|^2$ for any antenna in an enclosure will take the spectral form of equation (7).

For small enclosures or low frequencies, equation (7) will be characterized by discrete resonances, that are well separated in frequency. Under such conditions it becomes practical to curve fit equation (7) to the measured S_{11} and obtain the *Q* for each of the resonance frequencies, as shown in Fig. 1.

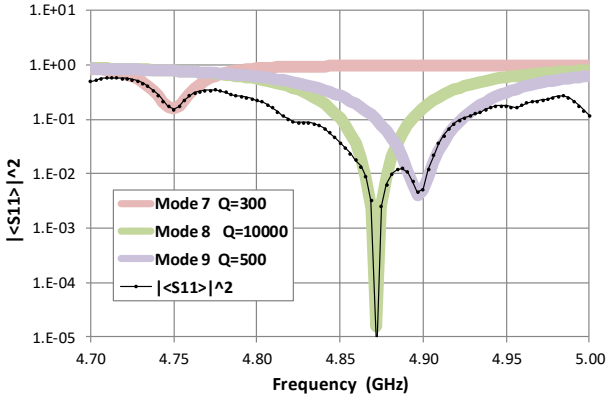

Fig. 1 Curve fit of eqn. (7) to the measured S_{11} for an antenna in an avionics box, quantifying the different Q factors for three modes

IV. Test Configuration

The small enclosure in which the measurements were performed is shown in Fig. 2. The resonant cavity was formed by a rectangular aluminum enclosure of internal dimensions 30 cm by 30 cm by 12 cm. A number of different aperture configurations were tested. This paper reviews the results of two configurations; a rectangular aperture of dimension 15 cm by 6 cm ("AP2" shown in Fig. 2) and a "closed box", where the aperture was covered with conductive tape.

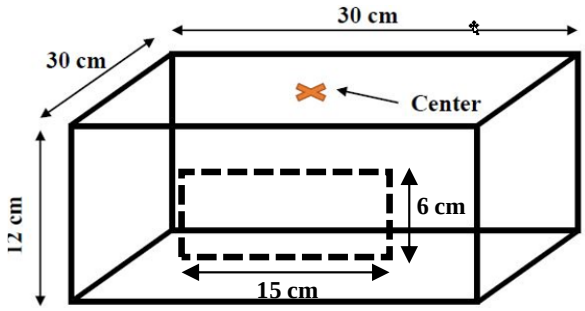

Fig. 2 Test box dimensions and aperture AP2 dimensions; the yellow cross shows the location of wire antenna

A 104 mm short wire antenna (Fig. 3) with radius 0.41 mm was fed through the enclosure wall by an N-type connector.

Fig. 3 The 104 mm short wire antenna

Additional, comparison measurements were taken with a 30 cm long curved wire antenna (Fig. 4) installed with N-type connector, as suggested by Tait [7]

Fig. 4 The 30 cm long, curved wire antenna

V. TEST RESULTS

A. Time Domain Q Measurement

The one-port (S_{11}) technique of [10] was used to measure the Q due to small box dimension [12]. Use of a single antenna enables a measurement of the cavity with lower antenna loading. The probe location is shown with yellow cross in Fig. 2. The VNA transformed the time-domain response of the results from the frequency-domain S_{11} using a fast Fourier transform. A Kaiser-Bessel window was applied to the frequency-domain spectrum to avoid replication of the sampled signal, giving S_{11} the in time domain.

The measurement was performed at 50 tuner positions (7.2° step) with 1601 frequency samples collected by the VNA at each position. The VNA was connected to the probe feed connector to measure the S_{11} scattering parameter.

Once the time-domain responses have been found at each tuner position, all are averaged across the tuner positions to give a mean chamber time-domain response. A sample result is shown in Fig. 5. The $\Im[S_{11}]$ decay response was averaged over 4 different probe locations.

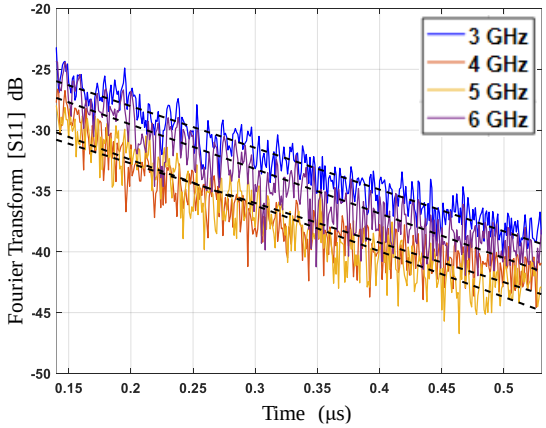

Fig. 5 Sample decay time results for the closed box condition

The measured Q results for the closed box and with aperture AP2 on the front face are shown in Table 1 and 2. The measurements show that the Q of the box with aperture AP2 is 8 dB lower than the fully covered box, as expected.

Table 1 Closed Box Q with no aperture

F (GHz)	3	4	5	6
Q (dB)	34.07	35.32	36.29	37.08

Table 2 Box Q with aperture AP2

F (GHz)	3	4	5	6
Q (dB)	26.43	27.68	28.65	29.44

B. Curvefitting <S_{11}> of the Wire Antenna

The S_{11} of the short wire antenna was first measured in the reverberation chamber, free of any box loading effects. The result is shown in Fig. 6 . The antenna exhibits good impedance matching at the standing wave resonance frequencies of the wire $f_n \approx \frac{c}{4L}, \frac{3c}{4L}, \frac{5c}{4L}, \frac{7c}{4L} \ldots$ (*0.72, 2.16, 3.6, 5.0 GHz*). For the over-moded reverberation chamber, there is no measurable difference between $\left|\langle S_{11}\rangle\right|^2$ and $\left\langle\left|S_{11}\right|^2\right\rangle$ indicating that the antenna impedance in the RC is the same as free field [2], [7].

Appling modal curve fitting to the measured short wire antenna $\left|\langle S_{11}\rangle\right|^2$ yields the Q of the antenna's standing wave resonances, shown overlaid in Fig. 6 . These modes have low Q factors, as their impedance at resonance matches the resonant impedance of the reverberant chamber modes. The reverberant chamber modes have high modal density *and high modal overlap*, to the point they are almost indistinguishable in the measured $\left|\langle S_{11}\rangle\right|^2$.

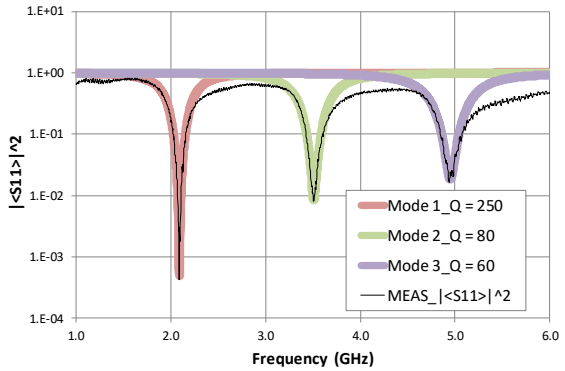

Fig. 6 Q factor of short wire antenna standing wave resonances obtained by cure-fitting equation (8).

When the same antenna S_{11} is measured in the small box, the result in Fig. 7 changes significantly. It exhibits reasonably good impedance matching at both the wire standing wave frequencies and certain box internal resonance frequencies. The narrower bandwidth at each resonance - compared with Fig. 6 - is attributable to the much lower modal overlap of box modes, compared with the modal overlap of RC modes.

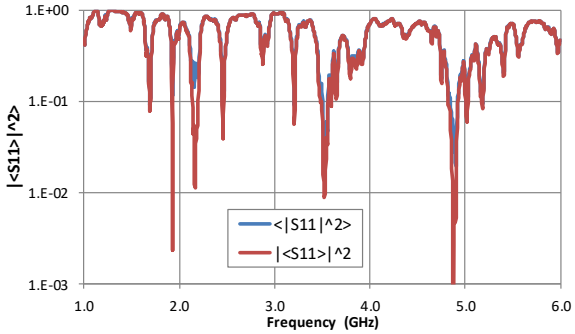

Fig. 7 S_{11} of the Short wire antenna, measured in the box enclosure with aperture AP2.

It can be seen from equation (7) that at each resonance frequency of the box $\omega = \omega_r$ the strength of the power radiated depends on three parameters; the antenna current magnitude $\left|I_\xi(j\omega)\right|$, the *spatial matching* between the antenna current distribution and the box resonant mode shape $\zeta_r(\omega) = \int_L \psi_r(\mathbf{x}_i) I_\xi(\mathbf{x}_i, \omega) d\mathbf{x}_i$, and the modal Q factor

$$P_{rad}(\omega_r) \propto \frac{Q_r \zeta_r}{\omega_r} \qquad (8)$$

The Q factor of the wire antenna can be expected to be higher than when tested in the RC, because the more widely spaced resonances in the small enclosure no longer closely align (or over-lap) with the wire standing wave resonances.

The corresponding measured S_{11} for the long wire shown in Fig. 8 confirms equation (8). The longer, curved wire couples with more of the box modes, and supports more of its own complex surface modes.

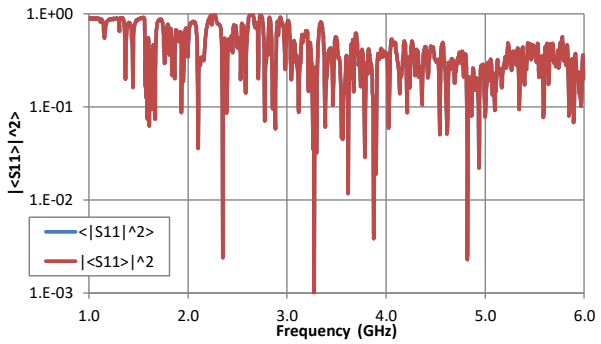

Fig. 8 S_{11} of the long wire antenna, measured in the box enclosure with aperture AP2.

The result of curve-fitting equation (7) to both short and long wire S_{11} to obtain "modal Q" estimates is shown in Fig. 9. The results show significant variance in the modal Q, consistent with equation (8). Both sets of modal Q results are generally consistent with the frequency band integrated results from the "T60 decay" time domain measurement. The longer wire - with a larger sample of participating modes - shows the best agreement.

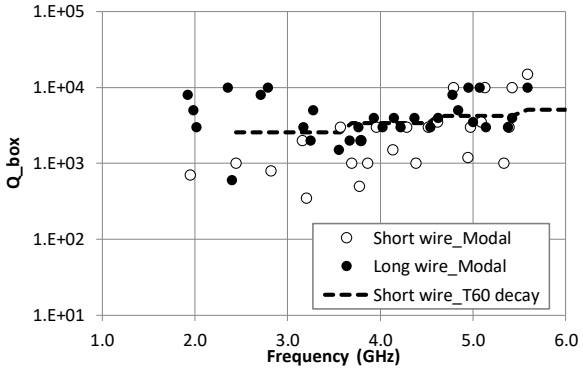

Fig. 9 Modal Q of the closed box, measured with short and long wire antenna; compared with T60 time decay result.

The corresponding long wire modal Q results for the small enclosure with aperture AP2 is shown in Fig. 10.

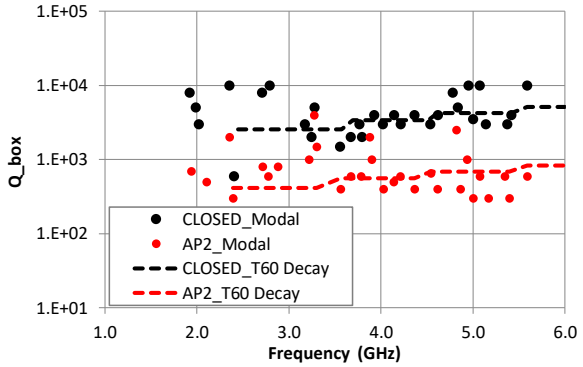

Fig. 10 Modal Q of the box with aperture AP2, measured with long wire antenna; compared with T60 time decay results.

For the small enclosure with aperture AP2, S_{11} measurements were taken at two addition locations to

determine sensitivity to the box mode shape coefficient $\psi_r(\mathbf{x}_i)$

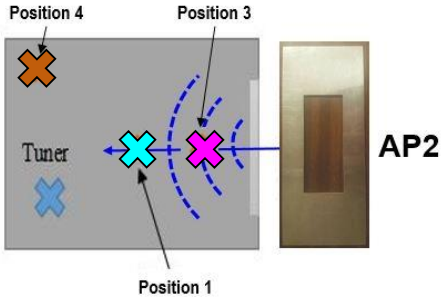

Fig. 11 Three different <S11> measurement locations in box with aperture AP2.

The S_{11} results in Fig. 12 show a significant variation in the amplitude of each resonance at different locations, consistent with equation (8). However, equation (7) suggests the shape of the resonance response - controlled by modal loss factor $\eta_r \equiv Q_r^{-1}$ - will be the same in all three locations.

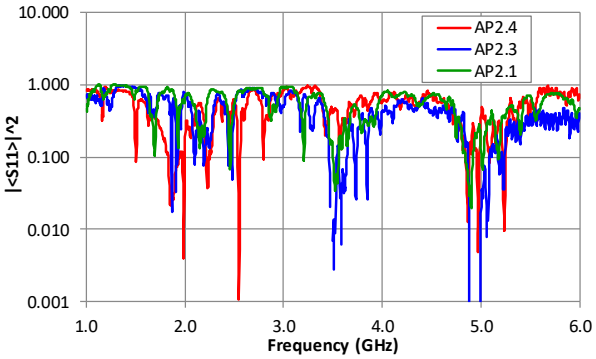

Fig. 12 S_{11} of the short wire antenna, measured in the AP2 aperture enclosure at three locations

Curve fitting equation (7) to the short wire $\langle |S_{11}|^2 \rangle$ measurements in the AP2 aperture enclosure (Fig. 12) yielded the estimates of modal Q shown in Fig. 13 .

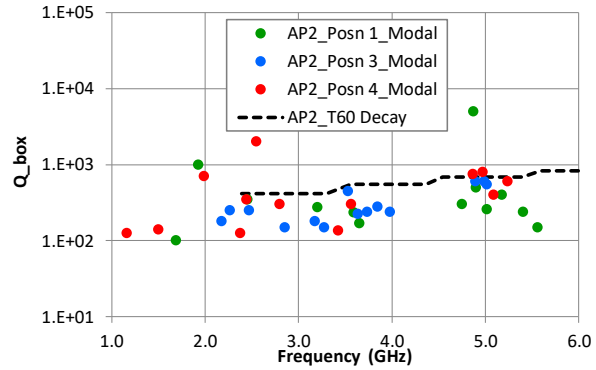

Fig. 13 Modal Q of the box with aperture AP2, measured at 3 wire positions; compared with T60 time decay results.

These results indicate that the modal Q measurement process is not strongly influenced by measurement location, even with only limited mode sampling using the short wire. This is consistent with equations (7) and (8).

VI. Predicted Q Factors

The small enclosure Q due to wall losses was calculated [1]

$$Q_{wall} = \frac{3V_c}{2\mu_r \delta_w A_w} \qquad (9)$$

$$\delta_w = 2/\sqrt{\omega \mu_w \sigma_w}$$

The Q due antenna loss was calculated [1] as

$$Q_{ant} = \frac{16\pi^2 V_c}{\left(1 - |\langle S_{11} \rangle|^2\right)\lambda^3} \qquad (10)$$

where for an ideal matched antenna, $|\langle S_{11} \rangle|^2 = 0$

For the large rectangular aperture AP2 with length l_2 and width w_2, the aperture Q was estimated assuming an equivalent circular radius [1] of $a = l_2/2$, but only for waves incident over a limited azimuth $\theta_2 \approx \tan^{-1}(w_2/l_2)$ as follows

$$Q_{AP2} = \frac{8|\theta_2|V_c}{\lambda} \begin{cases} \dfrac{9\pi}{16k^4a^6} & ka < 1.3 \\ \dfrac{2}{\pi a^2} & ka \geq 1.3 \end{cases} \qquad (11)$$

The predicted Q results (assuming ideal antenna) are shown overlaid with modal curve fit results for both closed and AP2 apertures, in Fig. 14 . There is good agreement at frequencies above 3 GHz.

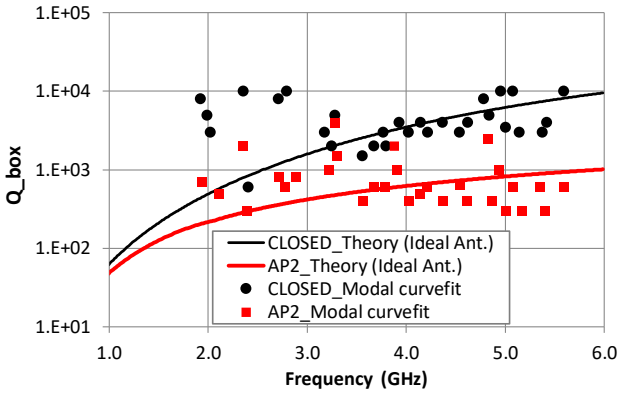

Fig. 14 Predicted box Q for both closed and AP2 apertures; compared with Modal Q curve-fit to measured S_{11}.

The deviation of modal Q test results from theory below 3 GHz is largely attributable to the impedance mismatch of the wire antenna (both short wire and long wire), compared with an ideal antenna. The contribution of antenna impedance mismatch to the determination of modal Q is evaluated by using measured $|\langle S_{11} \rangle|^2$ in equation (10), as shown in Fig. 15. This explains the scatter in modal Q, measured below 3 GHz.

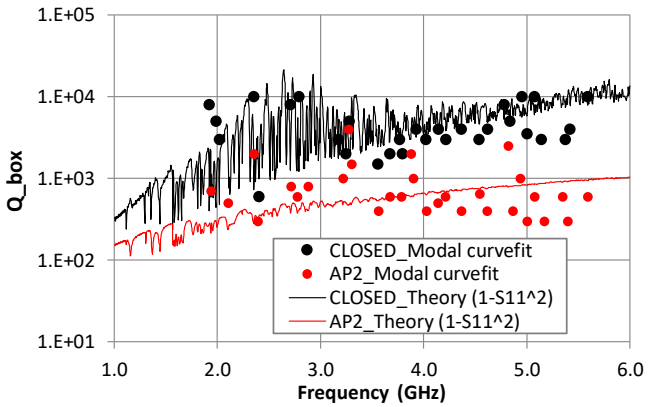

Fig. 15 Predicted box Q corrected for wire antenna impedance mismatch, compared with Modal Q curve fit to measured S_{11}.

VII. Modal Overlap of the Small Enclosure

Reliable prediction of Q allows calculation of the modal overlap of a small enclosure. Predictions for the test box with closed and AP2 apertures is shown in Fig. 16. In both cases, modal overlap asymptotes to unity at low frequency, if there is an ideal (perfectly matched) antenna in the enclosure. The closed box modal overlap remains near unity at higher frequencies, because the antenna loss $\eta \propto \omega^{-3}$ in eqn. (10) is greater than wall losses, offsetting the ω^2 increase in modal density. Adding aperture losses (or other controlled losses, such as absorbent material inside the box) results in an increase in modal overlap with frequency, as shown for aperture AP2.

However, in a real avionics (electronics) box, the effective antenna loss is provided by power traces or signal traces on circuit boards with matching load impedance. These conductors will be more like the short and long wires tested in this study, in which case the modal overlap is likely to be less than unity, leading to under-moded statistics.

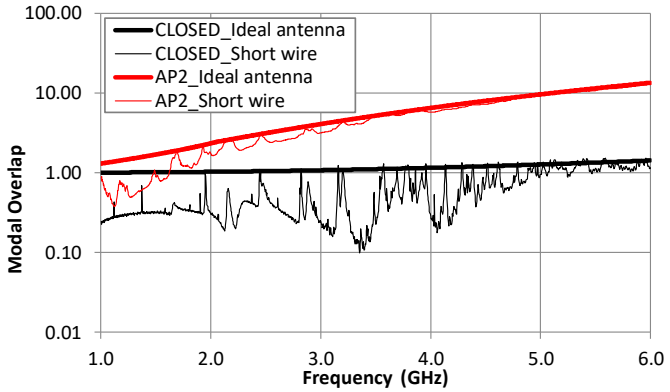

Fig. 16 Modal overlap of the small box enclosure, showing the influence of impedance mismatch of the wire antenna.

Understanding the effect of this predictable modal overlap on the mean and maximum expected electric field response in electrically small enclosures is the subject of continuing research by the authors.

VIII. Conclusion

The use of modal overlap has been suggested as a more definitive parameter for defining the under-moded condition in electrically small enclosures. Calculation of modal overlap requires reliable measurement and prediction methods for Q factor. The measurement of Q in small under-moded enclosures has be shown to be possible using the time-domain methods developed for over-moded revereberation chambers. In addition, a modal curefitting method has been introduced and shown to be consistent, for under-moded enclosures with well-separated modes (ie. low modal overlap).

These findings improve the aerospace community's ability to predict the EMC radiated immission performance of electronics components in avionics boxes. The Q factor controls the mean shielding effectiveness and it is anticipated that the modal overlap controls the maximum expected field strength.

References

[1] D. A. Hill, "Electromagnetic Fields in Cavities. Deterministic and Statistical Theories" John Wiley & Sons, Hoboken, New Jersey 2009

[2] J. Ladbury, G. Koepke, and D. Camell, "Evaluation of the NASA Langley Research Center Mode-Stirred Chamber Facility," NIST, Technical Note 1508, 1999.

[3] A. Schaffar and P. N. Gineste, "Application of the power balance methods to E- field calculation in the ARIANE 5 launcher payloads cavities," Presented at International Symposium on EMC, Long Beach, 2011, pp. 284-289.

[4] D.H. Trout, "Electromagnetic Environment in Payload Fairing Cavities," Dissertation, University of Central Florida, 2012.

[5] L. Kovalevsky, R.S. Langley, P. Besnier and J. Sol, "Experimental validation of the Statistical Energy Analysis for coupled reverberant rooms", Proc. IEEE Intnl. Symp. EMC, Dresden, August 2015

[6] Bremner, P.G, Vazquez, G., Trout, D.H and Cristiano, D.J., "Canonical Statistical Model for Maximum Expected Imission of Wire Conductor in an Aperture Enclosure", Proc. IEEE Intnl. Symp. EMC, Ottawa, October m2016

[7] G.B Tait, C. Hager, M.B. Slocum and M.O. Hatfiled, "On Measuring Shielding Effectiveness of Sparsely Moded Enclosures in a Reverberation Chamber", IEEE Trans. on EMC, Volume:55, Issue: 2, October 2012

[8] IEC, "Electromagnetic compatibility (EMC) – part 4-21: Testing and measurement techniques – Reverberation chamber test methods," Intnl. Electro technical Commission, Tech. Rep. IEC 61000-4-21, 2003

[9] Besnier, P., Lemoine, C. and Sol, J. "Various Estimations of Composite Q-factor with Antennas in a Reverberation Chamber", Proc. IEEE EMC Symp., Dresden, October 2015

[10] R. E. Richardson, "Reverberant microwave propagation," Naval Surface Warfare Center - Dahlgren Division, Dahlgren, Virginia, 22448-5100, Tech. Rep. NSWCDD/TR-08/127, 2008.

[11] J. M. Drozd and W. T. Joines, "Determining q using s parameter data," IEEE Trans. Microwave Theory Tech., vol. 44, no. 11, pp. 2123–2127, Nov. 1996.

[12] Nourshamsi, N., West, J.C. and Bunting, C.F., "Required Bandwidth for Time-Domain Measurement of the Quality Factor of Reverberation Chambers", Proc. IEEE Intnl. Symp. EMC, National Harbor,Maryland, October 2017

[13] T. H. Lehman, "A Statistical Theory of Electromagnetic Fields in Complex Cavities," Interaction Notes, USAF Phillips Laboratory, Note 494, May 1993

[14] P.G. Bremner, "Modal Expansion Basis for Statistical Estimation of Maximum Expected Field Strength in Enclosures", Proc. IEEE EMC Symposium, Santa Clara, March 2015

[15] Jason B. Coder, John M. Ladbury, Christopher L. Holloway and Kate A. Remley, "Examining the true effectiveness of loading a reverberation chamber: How to get your chamber consistently loaded", Proc. IEEE EMC Symposium., July 2010

[16] R.H. Lyon, Statistical analysis of power injection and response in structures and rooms", Jnl. Acoust. Soc. Amer. (1969) 45(3), 545-565.